

# Intracellular Routing and Inhibitory Activity of Oligonucleotides Containing a KDEL Motif

CHANTAL PICHON, KHALIL ARAR,<sup>1</sup> ALISTAIR J. STEWART,<sup>2</sup> MADELEINE DUC DODON, LOUIS GAZZOLO, PIERRE J. COURTOY, ROGER MAYER, MICHEL MONSIGNY, and ANNIE-CLAUDE ROCHE

*Glycobiologie Centre de Biophysique Moléculaire-CNRS and Université d'Orléans, F-45071 Orléans Cedex 02, France (C.P., K.A., A.J.S., R.M., M.M., A.-C.R.), Laboratoire d'Immuno-Virologie Moléculaire et Cellulaire, UMR 30 CNRS, Faculté de Médecine Alexis Carrel, F-69372 Lyon, France (M.D.D., L.G.), and Cell Biology Unit, Louvain University Medical School, UCL75.41, B-1200 Bruxelles, Belgium (P.J.C.)*

Received September 9, 1996; Accepted November 7, 1996

## SUMMARY

On internalization, oligonucleotides (ODN) remain mostly sequestered in endocytic compartments. To increase their delivery into the cytosol and/or nucleus, which contain their targets, we attempted to guide them into compartments containing the KDEL receptor. Antisense ODN, phosphodiester protected at both ends, that are complementary to the AUG initiation site of *gag<sub>HIV-1</sub>* mRNA (odn) were linked to a peptide ending with the Lys-Asp-Glu-Leu (KDEL) motif in a carboxyl-terminal position (odn-p-KDEL) or with the Lys-Asp-Glu-Ala (odn-p-KDEA) as a control. The effect of odn substitution with a peptide was examined with regard to its accumulation, subcellular location, and activity in HepG2 cells. Although odn-p-KDEL was internalized 4-fold less than the corresponding peptide-free odn, it was 5-fold more efficient in inhibiting *gag<sub>HIV-1</sub>* gene expression in HepG2 cells. The internalization of odn-p-KDEA was as low

as that of odn-p-KDEL, but its biological activity was lower, close to that of the peptide-free odn. On endocytosis at 37°, both conjugates as well as the peptide-free odn were found in a neutral environment. However, the substitution of an odn with a KDEL motif altered its intracellular trafficking; most of the odn-p-KDEL was found in the endoplasmic reticulum and in the intermediate compartment as identified by colabeling with either anti-ERGIC-53 or anti-KDEL receptor antibodies. Conversely, odn-p-KDEA and peptide-free odn were localized in vesicular compartments not labeled with these antibodies. In addition, pulse-chase experiments showed that odn-p-KDEL and odn-p-KDEA had a lower efflux than peptide-free odn. Therefore, the large increase in efficiency was due to the KDEL motif.

During the past decade, antisense ODN have been considered a new generation of putative therapeutic agents (1, 2). The use of conventional phosphodiester ODN was, however, limited for two main reasons: their high sensitivity to nucleases and their poor penetration into cells. To increase ODN stability, various chemical modifications have been designed (for a review, see Ref. 3). To increase cell penetration through plasma membrane, ODN have been associated with cationic lipids (4), covalently substituted with hydrophobic components (5), linked to poly-L-lysine (6), or embedded into antibody-tagged liposomes (7). Antisense ODN have been successfully used to inhibit expression of specific genes within

cells (2, 8) and viral genes, including Rous sarcoma virus (9) and HIV (10, 11).

We designed phosphodiester ODN/neoglycoprotein conjugates (12, 13); ODN, substituted at both ends to avoid exonuclease degradation, were further bound via a disulfide bridge to a glycosylated carrier to help them be efficiently internalized by cells expressing membrane lectins. Such glycoconjugates increased the cell uptake of ODN as well as their biological activity. However, both conventional and targeted ODN were indeed mainly confined into vesicular compartments; unfortunately, to be efficient, ODN must leave these vesicular compartments and reach the cytosol and/or the nucleus, the locations of their targets. The mechanism by which a small fraction of internalized ODN crosses the vesicle membranes and reaches the cytosol is not yet known. We postulated that the efficiency of ODN could be improved through modification of their intracellular trafficking to both avoid delivery to lysosomes and route them toward the ER,

This work was supported by grants from the Agence Nationale de Recherches sur le SIDA. K.A. received a fellowship from the Ministère de la Recherche et de la Technologie, and A.S. was supported by a postdoctoral fellowship from the Agence Nationale de Recherches sur le SIDA.

<sup>1</sup> Current affiliation: Sératec, F-93800 Epinay sur Seine, France.

<sup>2</sup> Current affiliation: Xenova Ltd., Slough SL1 4EF, UK.

**ABBREVIATIONS:** ODN, oligonucleotide(s); odn, phosphodiester oligonucleotide(s) (25-mer) complementary to the AUG initiation site of *gag<sub>HIV-1</sub>*; ER, endoplasmic reticulum; PBS, phosphate-buffered saline; FBS, fetal bovine serum; DMEM, Dulbecco's modified Eagle's medium; BSA, bovine serum albumin; HIV, human immunodeficiency virus; IC, intermediate compartment; odn-p-KDEL, oligonucleotide substituted with a peptide containing a KDEL motif; odn-p-KDEA, oligonucleotide substituted with a peptide containing a KDEA motif; TGN, *trans*-Golgi network; F-odn, fluoresceinylated odn.

from which they could presumably be more efficiently translocated into the cytosol and from which less would be released through regurgitation.

It is known that a carboxyl-terminal tetrapeptide KDEL motif mediates the retrieval of ER luminal proteins from the Golgi apparatus (14). Receptors recognizing the KDEL motif are located in the Golgi, IC, and ER (15, 16) and shuttle between those compartments.

The addition of a KDEL peptide or a related motif to the carboxyl terminus of bacterial and plant toxins increases their cytotoxicity (17, 18), presumably by allowing their retrograde transport through the Golgi apparatus into the ER (19). Toxin translocation into the cytosol could occur in either the ER or the *cis*-Golgi stacks (17, 20) or be favored by continuous cycling between the ER and the Golgi complex (21). In one study, the addition of a nonfunctional analogue KDEA (Lys-Asp-Glu-Ala) peptide instead of the KDEL peptide was less efficient in increasing the cytotoxicity of the toxins (18).

We hypothesized that ODN bearing a KDEL motif should be routed into these compartments and more easily enter the cytosol via translocation throughout one of these membranes. Furthermore, because phosphodiester ODN were rapidly effluxed (22, 23), ODN substituted with the KDEL motif (odn-p-KDEL) should be retained within cells for a longer time. To test this hypothesis, we synthesized oligonucleopeptides: 5' and 3' blocked phosphodiester odn covalently linked to a peptide containing the KDEL motif in a carboxyl-terminal position (24). To assess the role of the KDEL signal sequence, the same odn were substituted with a peptide containing the KDEA motif (odn-p-KDEA), which does not act as an ER retention motif.

The activity of peptide-free odn complementary to the AUG initiation site of *gag<sub>HIV-1</sub>* gene and that of the corresponding odn-p-KDEL or odn-p-KDEA was assessed in HepG2 cells transfected with relevant plasmids. Laser confocal microscopy analysis of HepG2 cells incubated with odn, odn-p-KDEA, and odn-p-KDEL substituted with a fluorescent tag was performed; intracellular compartments were identified through simultaneous labeling with antibodies against specific marker proteins. We found that the substitution of phosphodiester odn with a KDEL motif effectively targeted these conjugates to the appropriate compartments (ER, IC, and Golgi) and increased the inhibition of gene expression, whereas the peptide-free odn and the odn substituted with an inactive peptide (odn-p-KDEA) were not located into those compartments and were comparatively less efficient.

## Materials and Methods

### Cells

Human hepatoma HepG2 cells were obtained from American Type Culture Collection (8055 HB, Rockville, MD). Cells were maintained in DMEM (GIBCO, Refrewshire, Scotland) supplemented with 2 mM L-glutamine and antibiotics (100 units/ml penicillin and 100 µg/ml streptomycin, Eurobio, Paris, France) and 10% heat-inactivated FBS (GIBCO). They were grown at 37° in a humidified atmosphere containing 5% CO<sub>2</sub>/95% air. Cells were passaged on harvest of exponentially growing cells with PBS, pH 7.4, containing 0.5 mg/ml trypsin and 0.5 mM EDTA.

### Peptides

The peptide GEEDTSEKDEL, corresponding to the carboxyl-terminal sequence of the ER resident luminal protein GRP 78 (25), and the control peptide GEEDTSEKDEA were prepared by solid-phase synthesis on an Applied 433A peptide synthesizer (Applied Biosystems, Foster City, CA) by 9-fluorenylmethoxycarbonyl strategy. They were N<sub>α</sub>-substituted by a Cys(Npys) residue or by a bromoacetyl-tyrosine residue (24).

### The odn and the Oligonucleopeptides odn-p-KDEL and odn-p-KDEA

The odn chosen for this study was a phosphodiester odn complementary to the AUG initiation site of *gag* gene of HIV-1, odn<sub>gag</sub> and is referred to as odn. This odn was a pentacosanucleotide (25 mer): 5'-CTC TCG CAC CCA TCT CTC TCC TTC T-3' supplied by Eurogentec (Seraing, Belgium) or obtained from Dr. N. T. Thuong (CBM-Centre National de Recherche la Scientifique, Orleans, France). The 5' end was substituted with an alkyl dithiopyridine moiety, and the 3' end was substituted with an alkylamine: pyridyl-S-S-R<sub>1</sub>-5' (odn)3'-R<sub>2</sub>-NH<sub>2</sub>, where R<sub>1</sub> = (CH<sub>2</sub>)<sub>6</sub>-O-PO<sub>2</sub><sup>-</sup> and R<sub>2</sub> = PO<sub>2</sub><sup>-</sup>-O-(CH<sub>2</sub>)<sub>6</sub>. These modifications protect the phosphodiester oligodeoxynucleotide from exonuclease degradation and allow further substitution with fluorescent tags and/or peptides (24).

**Fluorescent conjugates.** The odn-S-S-pyridyl was reduced with 1 Eq of tris-(2-carboxyethylphosphine) in a thoroughly degassed buffer of 2 M sodium acetate and 0.1 M sodium phosphate buffer, pH 7.0; then, the 5' SH group was reacted with fluorescein iodoacetamide (*F*) or tetramethyl-rhodamine iodoacetamide (*R*) (Molecular Probes, La Jolla, CA). Alternatively, odn were labeled on their 3' NH<sub>2</sub> group by the use of fluorescein isothiocyanate. The fluorescent odn derivatives *F*-odn and *R*-odn were purified on Biogel P2 (BioRad, Ivry-sur-Seine, France), and their purity was checked with analytical high performance liquid chromatography on a reverse-phase 100 RP-18, 5-mm (250 × 4 mm) column (Merck, Darmstadt, Germany) using a linear gradient of 5–30% acetonitrile in 0.1 M triethylamine acetate, pH 7.0.

**Oligonucleopeptides.** The peptides GEEDTSEKDEL and GEEDTSEKDEA were coupled to the odn through a stable thioether linkage starting with an N<sub>α</sub>-bromoacetylpeptide to obtain odn-*Scm*-YGEEDTSEKDEL (*Scm* = thio-carboxymethyl), as previously described (24), or odn-*Scm*-YGEEDTSEKDEA. Oligonucleopeptide conjugates were purified by reverse-phase high performance liquid chromatography.

Peptides bearing a cysteinyl-thiopyridine residue were labeled as described above to obtain odn-*Smh*-C(*F*)GEEDTSEKDEL (*Smh* = thio-maleimido hexanoyl). In other cases, odn labeled on the 3'-alkylamine end was reacted on its 5' end with an N<sub>α</sub>-bromoacetylated peptide, leading to *F*-odn-*Scm*-YGEEDTSEKDEL or *F*-odn-*Scm*-YGEEDTSEKDEA.

Throughout the study, fluorophore-labeled odn (*F*-odn or *R*-odn) or oligonucleopeptides (*F*-odn-p-KDEL, *F*-odn-p-KDEA, or *R*-odn-p-KDEL) are abbreviated as *fl*-odn, *fl*-odn-p-KDEL, or *fl*-odn-p-KDEA, respectively.

**Radiolabeled odn.** Iodination of fluoresceinylated odn was achieved using iodogen reagent (Pierce, Paris, France). Briefly, iodogen-coated tubes were prepared by gently evaporating 400 µl of chloroform containing 500 µg/ml iodogen. *F*-odn, *F*-odn-p-KDEA, or *F*-odn-p-KDEL (100 µg in 100 ml) was added to iodogen-coated tubes followed by 5 µl of Na<sup>125</sup>I (Amersham, Paris, France; 581 MBq <sup>125</sup>I/mg). After 20 min, the reaction was stopped by transferring the reaction mixture to a tube containing 1 ml of ethanol. The precipitated radiolabeled odn were washed three times in ethanol. The odn were then suspended in 100 µl PBS, and the <sup>125</sup>I-incorporation was measured using a gamma counter (LKB, Paris, France).

## Biological Activity of Antisense odn and Oligonucleotides

**Transfection with pRET-luc plasmid.** The efficiency of antisense odn was monitored using a plasmid encoding the firefly luciferase reporter gene (*luc*) (pRET-*luc*, kindly provided by Dr. A. M. Aubertin, Strasbourg, France). This plasmid contains the luciferase reporter gene under the control of the human phosphoglycerate kinase promoter. The *luc* gene sequence around the AUG codon was replaced by the translation initiation site of *gag<sub>HIV-1</sub>* gene. Transfection was carried out by using lactosylated poly-L-lysine as previously reported (26). Briefly, HepG2 cells were plated onto 24 wells. After 1 day, cells were transfected with pRET-*luc* plasmid. DNA/lactosylated poly-L-lysine complexes were prepared by the addition (drop-wise and under constant mixing) of 25  $\mu$ g of lactosylated poly-L-lysine in 0.3 ml of DMEM to 10  $\mu$ g of pRET-*luc* plasmid in 0.7 ml of DMEM; the solution was then kept for 30 min at 20°. The solution containing the plasmid/polymer complexes was diluted by the addition of 1 ml of DMEM supplemented with 1% FBS (Sigma Chemical, St. Louis, MO), and chloroquine (100  $\mu$ M final concentration) was added. Four hours later, the medium was removed, and cells were further incubated 24 hr at 37° in a fresh medium (10% FBS) in the presence or absence of odn or oligonucleotides (odn-p-KDEA or odn-p-KDEL). Then, the medium was changed and replaced with fresh medium containing the same concentration of odn or oligonucleotide for 24 hr before measurement of the luciferase activity.

**Luciferase assay.** Luciferase gene expression was measured by luminescence (27). Cells were washed three times with PBS. The homogenization buffer [200  $\mu$ l of 8 mM MgCl<sub>2</sub>, 1 mM dithiothreitol, 1 mM EDTA, 15% glycerol (Prolabo, Paris, France), 25 mM Tris phosphate buffer, pH 7.8, 1% Triton X-100 (Sigma Chemical, Rouen, France) was added to each well, and the tissue culture plates were kept for 15 min at 20°. An aliquot of the supernatant (60  $\mu$ l) was mixed with 95  $\mu$ l of 2 mM ATP in the homogenization buffer without Triton X-100 and vortexed. Luminescence was recorded for 4 sec using a luminometer (LUMAT LB 9501, Berthold, Wildbach, Germany) on the addition of 150  $\mu$ l of 167 mM luciferin in water.

## Flow Cytometry Analysis

Plated HepG2 cells were incubated at 37° with *F*-odn, *F*-odn-p-KDEA, or *F*-odn-p-KDEL. After a 2-hr incubation, cells were washed three times with cold PBS containing 10 mg/ml BSA (PBS-BSA). To remove cell surface bound fluoresceinylated odn, 5  $\mu$ M SdC28 [a 28-mer phosphorothioate homopolymer of cytidine used to remove odn (28) from the cell surface] were added twice for 5 min at 4°. After washing, cells were harvested and resuspended in sheath fluid (134 mM NaCl, 3.75 mM KCl, 15.2 mM NaF, 1.9 mM KH<sub>2</sub>PO<sub>4</sub>, 16.5 mM NaHPO<sub>4</sub>, 0.2% 2-phenoxyethanol, pH 7.4). The cell fluorescence intensity was measured after a postincubation for 30 min at 4° in the absence or presence of 50  $\mu$ M monensin (Calbiochem, La Jolla, CA). This ionophore neutralizes endocytic compartments and thereby retrieves fluorescence from acid quenching (29). Cell fluorescence intensities were measured using a FACS analyzer (Becton Dickinson, Sunnyvale, CA) equipped with a FACSlite unit (Becton Dickinson) and was expressed as mean values from triplicate experiments; data shown are the mean values from 5000 cells obtained with the use of Cell Quest Software (Becton Dickinson). A 488-nm excitation wavelength was produced by a 25-mW cold-air argon laser. The signal was assessed relative to that of calibrated fluorescent beads (30).

## Efflux of Radiolabeled odn

HepG2 cells seeded onto 24-well plates ( $2 \times 10^5$  cells/well) were incubated at 37° for 2 hr in complete medium containing 4  $\mu$ M <sup>125</sup>I-labeled odn, <sup>125</sup>I-labeled odn-p-KDEA, or <sup>125</sup>I-labeled odn-p-KDEL (3 GBq/mol). Cells were extensively washed to remove odn from cell surface as described above, and they were further incubated for the indicated period of time in fresh medium. Then, cells were harvested by treatment with PBS containing 0.2 mg/ml EDTA and

2.5  $\mu$ g/ml trypsin and washed with PBS before lysis in 0.1 N NaOH. Radioactivity was measured using a gamma counter (LKB), and protein content was determined according to the Lowry method (31).

## Laser Scanning Confocal Microscopy Analysis

**Localization of peptide-free odn and of oligonucleotides.** HepG2 cells ( $2 \times 10^5$ /well) were plated onto glass coverslips and cultured for 24 hr. After washing, cells were incubated in DMEM supplemented with 10% FBS for 2 hr at 37° with 7.5  $\mu$ M odn, odn-p-KDEA, or odn-p-KDEL labeled with a fluorescent tag. After three washes with PBS containing 10 mg/ml BSA at 4°, cells were fixed with 3% *p*-formaldehyde (Merck, Darmstadt, Germany) in PBS for 20 min at 37°, incubated in a 50 mM NH<sub>4</sub>Cl solution to block residual aldehyde groups, and mounted in a PBS/glycerol mixture (v/v) containing 1% 1,4 diazo bicyclo-(2,2,2)-octane as an antifading agent (32). Cells were analyzed with a confocal imaging system (MRC-600, BioRad) equipped with a Nikon Optiphot epifluorescence microscope (Nikon, Tokyo, Japan) and a 60 $\times$  Planapo objective (numerical aperture, 1.4). A krypton/argon laser tuned to produce both 488-nm fluorescein excitation and 565-nm rhodamine excitation wavelength beams allowed simultaneous reading of both fluorescent signals and image merging. Diaphragm and fluorescence detection levels were adjusted to reduce to a minimum any interference between fluorescein and rhodamine channels. Pictures were recorded with a Kalman filter (average of 10–15 images).

**Localization of odn, ERGIC-53, and the compartments containing KDEL receptors.** On a 2-hr pulse with *fl*-odn, *fl*-odn-p-KDEL, or *fl*-odn-p-KDEA at 37°, cells were washed and further incubated in fresh medium at 15° for 3 hr. Then, they were processed for immunolabeling using an anti-ERGIC-53 antibody (ERGIC-53 is a protein specific to the IC between the ER and the Golgi apparatus) (kindly provided by Dr. H. P. Hauri, Biozentrum, Basel, Switzerland) or with an anti-KDEL receptor antibody (kindly provided by Dr. B. Tang, Institute of Molecular and Cell Biology, National University of Singapore, Singapore). After extensive washing in PBS containing 10 mg/ml BSA, cells were fixed by incubation in 30 mg/ml *p*-formaldehyde and 0.1% glutaraldehyde (Merck) in PBS for 1 hr at 37° followed by a 10-min incubation at room temperature in 50 mM NH<sub>4</sub>Cl and then permeabilized with 1 mg/ml saponin in PBS for 15 min at room temperature. Cells were incubated for 1 hr with a specific antibody and then with a secondary anti-isotype antibody labeled with a fluorophore.

## Results

**Biological effect.** The inhibitory effects of antisense phosphodiester odn, protected at both 5' and 3' ends, directed against the AUG initiation site *gag<sub>HIV-1</sub>* and of two derived oligonucleotides [odn-p-KDEL (odn-*Scm*-YGEEDTSEKDEL) and odn-p-KDEA (odn-*Scm*-YGEEDTSEKDEA)] was tested in HepG2 cells. These cells were chosen because they are suitable for infection by HIV (33). The odn or the oligonucleotides were added to HepG2 cells, which had been transfected by incubation for 4 hr with pRET-*luc* plasmid complexed with lactosylated poly-L-lysine, and the luciferase activity was determined 48 hr later. Because the sequence around the AUG codon site of the luciferase gene was replaced by the sequence surrounding the initiation translation site of *gag<sub>HIV-1</sub>* gene, the luciferase activity was expected to be inhibited by antisense odn complementary to this gag target sequence. The odn-p-KDEL was 5- and 3.5-fold more efficient than the peptide-free odn and the odn-p-KDEA, respectively. Indeed, the IC<sub>50</sub> value for odn-p-KDEL was  $0.20 \pm 0.05$   $\mu$ M compared with  $1.0 \pm 0.2$   $\mu$ M for the peptide-free odn and  $0.7 \pm 0.1$   $\mu$ M for the odn-p-KDEA. At 2  $\mu$ M, a



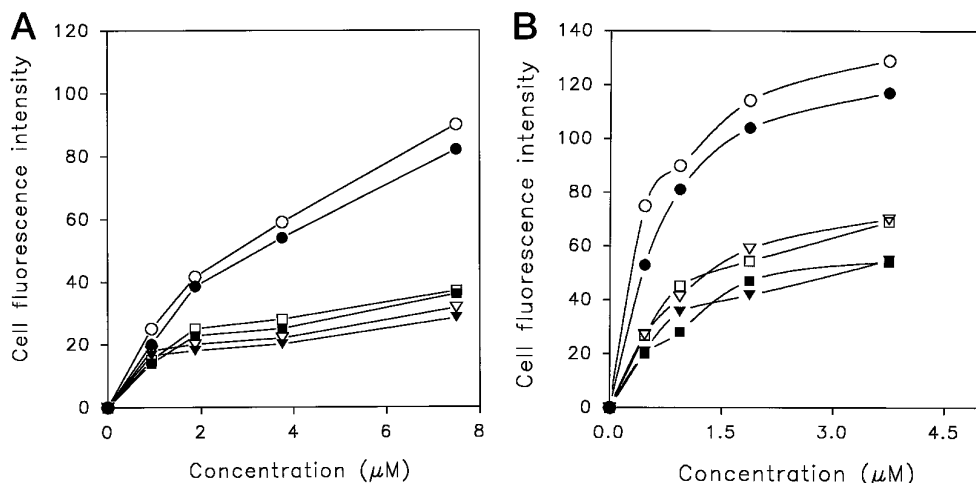


**Fig. 1.** Uptake of odn, odn-p-KDEA, and odn-p-KDEL. HepG2 cells were incubated at 37° for 2 (A) or 24 (B) hr in the presence of the indicated concentrations of *F*-odn (●, ○), *F*-odn-p-KDEA (▼, ▽), or *F*-odn-p-KDEL (□, ■). Cell fluorescence intensities (arbitrary units) were measured by flow cytometry after a postincubation period of 30 min at 4° without (●, ▼, ■) or with (○, ▽, □) 50  $\mu$ M monensin as described in Materials and Methods.

comparable 80% inhibition was obtained with both free odn and oligonucleotides.

**Cell uptake and efflux.** Flow cytometry analysis was performed to determine whether the highest activity of the odn-p-KDEL could be related to an uptake increase. We used identical fluorescent derivatives (*F*-odn, *F*-odn-p-KDEA, and *F*-odn-p-KDEL) with the same fluorescence emission intensity. After a 2- or 24-hr incubation at 37° with different concentrations of these derivatives, fluorescent odn adsorbed on the cell surface were released after a post-treatment at 4° in the presence of SdC28. The amount of the endocytosed material was determined by measuring the cell-associated fluorescence intensity. As reported by Stein *et al.* (28), SdC28 efficiently competes for phosphodiesterases as well as phosphorothioates. The cellular uptake of odn and oligonucleotides was concentration dependent up to 4  $\mu$ M and approximately twice as high after a 24-hr incubation compared with a 2-hr incubation. However, the level of uptake of *F*-odn-p-KDEL and *F*-odn-p-KDEA was 4-fold lower than that of *F*-odn after both incubation time periods (Fig. 1, A and B). A post-treatment with 50  $\mu$ M monensin induced only marginal increase of cell fluorescence in any cases, indicating that both odn and oligonucleotides (odn-p-KDEL or odn-p-KDEA) were essentially localized in poorly acidified compartments.

To investigate whether oligonucleotides (odn-p-KDEL and odn-p-KDEA) had a different efflux than peptide-free odn, we used iodinated odn in pulse-chase experiments. HepG2 cells were incubated in the presence of 4  $\mu$ M  $^{125}$ I-labeled *F*-odn, *F*-odn-p-KDEA, or *F*-odn-p-KDEL (3 GBq/mol) at 37° for 2 hr. After removal of the cell surface-bound odn with SdC28, cells were further incubated with odn-free medium for different periods of time. These experiments confirmed the results obtained by flow cytometry analysis: at time 0 of chase, the intracellular odn accumulation was higher than that of odn-p-KDEA or odn-p-KDEL (Fig. 2). After a 3-hr chase, 80% of the oligonucleotides (odn-p-KDEL and odn-p-KDEA) were retained in HepG2 cells, whereas only 30% of peptide-free odn remained associated with the cells. Similar results were obtained with 6-hr loading followed by 3 hr of chase (data not shown). Thus, the lower level of accumulated oligonucleotide cannot be attributed to a more rapid efflux and truly reflects a lower endocytic rate. In addition, odn substitution with peptides greatly affected cell retention, suggesting a different intra-

cellular routing. This could account for the higher activity of odn-p-KDEL despite a lower cell uptake than peptide-free odn. The fact that odn-p-KDEA was not as efficient as odn-p-KDEL despite comparable uptake and an efflux rate further suggests that intracellular routing involves the KDEL receptors.

**Intracellular localization.** The KDEL receptors mediating the retrieval of resident proteins are located in the IC as well as in the ER and the *cis*-Golgi apparatus (15, 16). To estimate the extent of association of odn-p-KDEL with the compartments containing the KDEL receptors, we used double labeling with monoclonal antibodies against ERGIC-53, a specific marker of the IC, or against the KDEL receptor. We further took advantage of the blockade of vesicular transport at 15° (34), a low temperature that slows down the retrograde part of the cycling pathway between the ER and the IC and

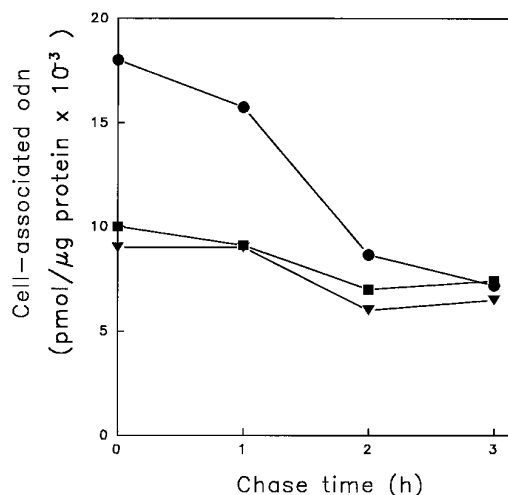


**Fig. 2.** Efflux of odn, odn-p-KDEA, and odn-p-KDEL. Cells in 24-well plates were incubated at 37° for 2 hr (pulse) in RPMI/10% FBS containing 4  $\mu$ M  $^{125}$ I-labeled *F*-odn (●),  $^{125}$ I-labeled *F*-odn-p-KDEA (▼), or  $^{125}$ I-labeled *F*-odn-p-KDEL (■) (3 GBq/mol). Then, medium was removed, and cells were further incubated at 37° in fresh medium for the time periods indicated (chase). Cells were harvested after washing as described in Materials and Methods. Radioactivity was measured using a gamma counter, and protein content was determined according to the Lowry method. Results are typical of experiments carried out in triplicate and repeated several times. Data are expressed as mean  $\pm$  standard deviation.

## Discussion

A main limitation to the activity of ODN is their inability to cross a lipid bilayer membrane. Indeed, odn are relatively high-molecular-weight polyanions and as such are not membrane permeant; on endocytosis, they essentially remain located inside vesicular compartments and only a small ODN fraction leaves the lumen by crossing the vesicular membrane and reaches its targets in the cytosol and the nucleus. On these bases, we decided to modify the ODN to guide them into deep internal compartments; only a small ODN fraction leaves the lumen by crossing the vesicular membrane and reaches its targets in cytosol and the nucleus. On these bases, we decided to modify the ODN to guide them into deep internal compartments, from where they could reach the cytosol more easily. In this study, we used phosphodiester ODN that were substituted at both ends to protect them from exonuclease degradation and to allow attachment of a tag and/or a peptide. The pentacosanucleotide directed against AUG *gag*<sub>HIV-1</sub> odn was substituted through a stable thioether bond to a peptide bearing a KDEL motif in the carboxyl-terminal end (24). As a control, we synthesized oligonucleotides with a peptide containing a KDEA motif. We found that antisense odn linked to a peptide with a carboxyl-terminal KDEL motif were more effective than the peptide-free odn, despite a lower uptake; furthermore, oligonucleotides bearing a KDEL motif were more efficient than the oligonucleotides bearing a KDEA motif that was taken up at a similar level. The odn-p-KDEL were efficiently targeted toward internal compartments containing the KDEL receptors and ERGIC-53, a protein of the IC.

The activity of the antisense odn was evaluated *in vitro* with HepG2 cells transfected with pRET-*luc* plasmid containing a sequence of the AUG initiation site of *gag*<sub>HIV-1</sub> gene encoding the luciferase gene. A significant improvement in the activity was obtained with the oligonucleotide odn-p-KDEL ( $IC_{50} = 0.2 \mu M$ ) compared with the peptide-free odn ( $IC_{50} = 1.0 \mu M$ ). The presence of alanine instead of leucine in the oligonucleotide abolished the benefit of the peptide substitution. Indeed, odn-p-KDEA was not as efficient as odn-p-KDEL ( $IC_{50} = 0.7 \mu M$ ). Similar results were obtained using odn-p-KDEL in HepG2 cells transfected with an HIV-1 molecular clone and in THP1 monocytic cells chronically infected with HIV-1<sup>3</sup> as well as in peripheral blood monocytes infected with the HIV-IIIB strain (24).

In contrast to the higher activity of odn-p-KDEL, the uptake of odn bearing a dodecapeptide that includes a carboxyl-terminal KDEL motif was 4-fold lower than that of the peptide-free odn. A lower cellular uptake was also observed with odn-p-KDEA. Because uptake of ODN involves adsorptive endocytosis (36, 37), this decrease could be related to either a lower cell surface binding or a lower uptake because the dodecapeptide increases the anionic character and the molecular mass of the conjugate. Efflux studies showed that the dodecapeptides improved cellular retention of both conjugates.

Thus, odn-p-KDEL is 5-fold more efficient than the peptide-free odn despite a lower uptake. We hypothesized that the addition of a peptide terminated with a KDEL motif

compacts the IC close to the Golgi apparatus in Vero cells (35). This phenomenon also occurred with HepG2 cells; indeed, the IC of HepG2 cells was distributed throughout the cytoplasm at 37°, whereas it became concentrated near the nucleus on incubation at 15° (data not shown).

A coinubation experiment with fluorophore-labeled odn and odn-p-KDEL for 2 hr at 37° (loading step) followed by a 3-hr chase at 15° (clustering step) showed that most of *fl*-odn-p-KDEL was located in the perinuclear area, whereas *fl*-odn-containing vesicles were scattered throughout the cytoplasm (Fig. 3). We determined that the localization of the odn as well as that of the oligonucleotides was independent on the nature of the added fluorophore (fluorescein or rhodamine).

Next, immunolabeling was performed to formally identify the intracellular compartments containing odn and oligonucleotides. Cells were incubated with *fl*-odn, or *fl*-odn-p-KDEA, or *fl*-odn-p-KDEL for 2 hr at 37° and then transferred to 15° for 3 hr before fixation, permeabilization, and immunolabeling with either the anti-ERGIC-53 antibody (Fig. 4) or the anti-KDEL receptor antibody (Fig. 5). After a 3-hr incubation at 15°, the *fl*-odn-p-KDEL was mainly observed in areas labeled with the anti-ERGIC-53 antibody, close to the nucleus (Fig. 4a), whereas *fl*-odn-p-KDEA (Fig. 4b) clearly showed a distinct localization (i.e., was essentially spread throughout the cytoplasm). Immunolabeling with an anti-KDEL receptor antibody confirmed the distinct localization of odn-p-KDEL. Indeed, odn-p-KDEL and the anti-KDEL receptor antibody distributions largely overlapped (Fig. 5c), whereas peptide-free odn (Fig. 5a) and odn-p-KDEA (Fig. 5b) were found in a localization distinct from that of the KDEL-receptor antibody.

If a chase was performed at 37° instead of 15°, odn-p-KDEL was still in compartments containing ERGIC-53 and the KDEL receptors, but the spreading was greater than that on incubation at 15° (data not shown).

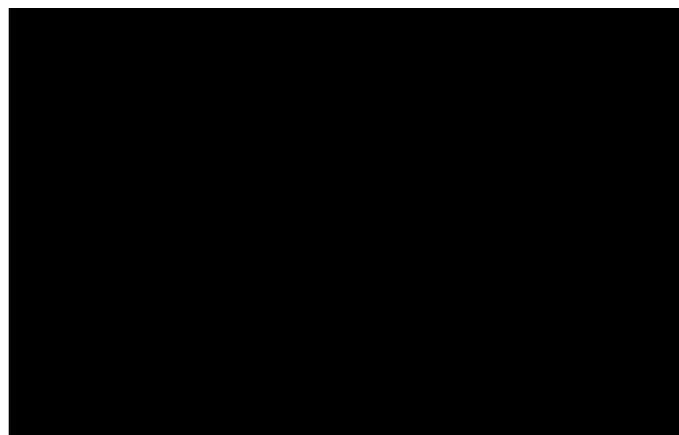


**Fig. 3.** Subcellular localization of odn and odn-p-KDEL on endocytosis at 37° followed by a postincubation period at 15°. HepG2 cells were incubated in the presence of both *F*-odn and *R*-odn-p-KDEL for 2 hr at 37°, washed, further incubated in fresh medium for 3 hr at 15°, and examined by confocal microscopy. The green and red fluorescence images were merged. In these representative optical medial sections, the *R*-odn-p-KDEL (red) was concentrated close to the nucleus, whereas the *F*-odn (green) was spread into vesicles throughout the cell. Scale bar, 10  $\mu m$ .

<sup>3</sup> C. Pichon, K. Arar, A. J. Stewart, M. Duc Dodon, L. Gazzolo, R. Mayer, M. Monsigny, and A.-C. Roche, unpublished observations.

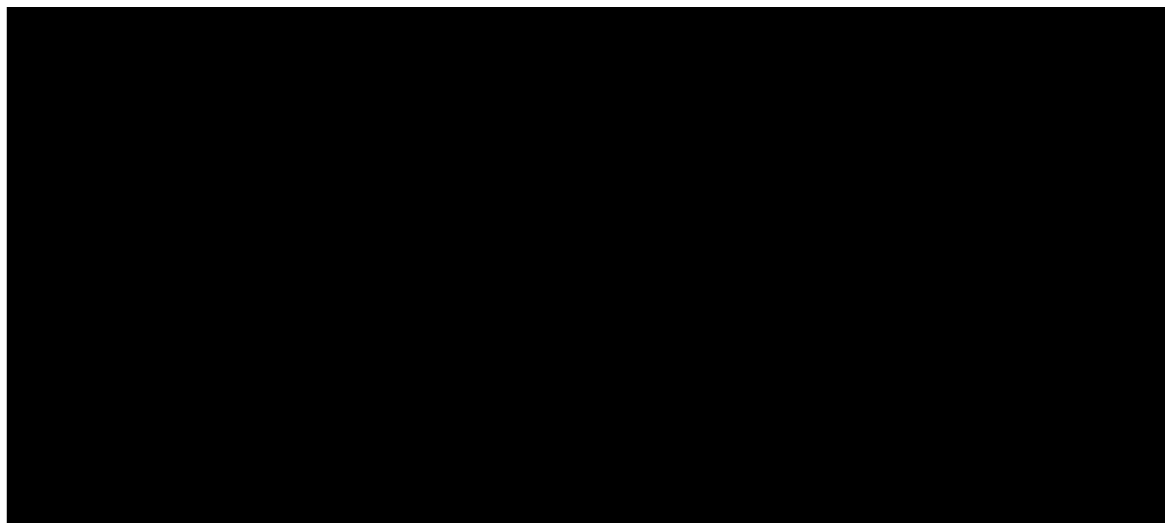


**Fig. 4.** Localization of odn-p-KDEA and odn-p-KDEL relative to compartments containing ERGIC-53. HepG2 cells were first incubated for 2 hr at 37° with either 7.5  $\mu$ M *R*-odn-p-KDEL (a) or *R*-odn-p-KDEA (b) and then further incubated for 2 hr at 15° before immunolabeling with anti-ERGIC-53 antibody. The localization of anti-ERGIC-53 antibody was demonstrated by the use of *F*-goat anti-mouse IgG (*green*); odn-p-KDEA and odn-p-KDEL are *red*. The green and red fluorescence images were merged. a, *Yellow* signals show that odn-p-KDEL were predominantly located in areas containing ERGIC-53. b, The absence of a *yellow* signal indicates the absence of codistribution. Scale bar, 25  $\mu$ m.

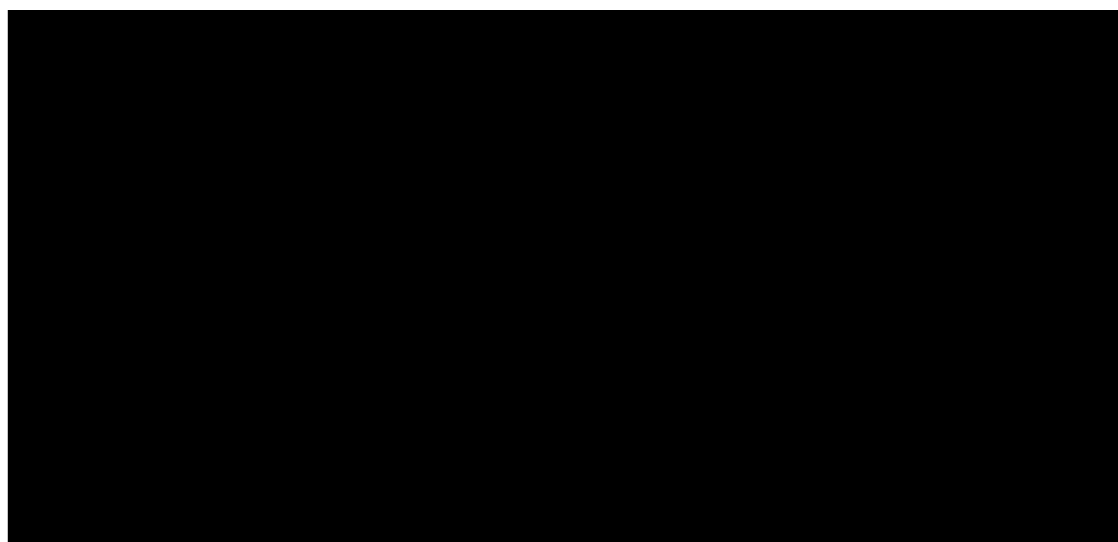


**Fig. 5.** Localization of odn, odn-p-KDEA, and odn-p-KDEL relative to compartments containing KDEL receptor. Cells were treated with *F*-odn (a), *F*-odn-p-KDEA (b), or *F*-odn-p-KDEL (c) as described in the legend to Fig. 4 except that immunolabeling was performed using an antibody against the KDEL receptor, which was demonstrated by the use of *R*-goat anti-mouse immunoglobulin (*red*). Odn, odn-p-KDEA, and odn-p-KDEL are *green*. No colocalization of odn and odn-p-KDEA with the KDEL receptor antibody was observed (a and b). c, Conversely, odn-p-KDEL and the KDEL receptor largely overlap. Scale bar, 25  $\mu$ m.

changed the routing of ODN and increased the ODN passage into the cytosol and/or nucleus, in which their targets are located. This hypothesis was supported by the lower efficiency of odn-p-KDEA, which suggests that the role of the KDEL motif is to target efficiently the odn in a more leaky compartment, allowing their translocation to the cytosol. It is, however, noticeable that despite a lower uptake (4-fold lower), odn-p-KDEA had an efficiency similar to that of the peptide-free odn. These data suggest that the peptide substitution by itself was able to induce an increased activity. This could be related to a longer cellular retention of this oligonucleotide.

Compartments containing odn were not actively acidified: the fluorescence intensity was not enhanced to a significant extent on monensin post-treatment at 4°. These results are in

agreement with those of Tonkinson and Stein (23), who showed that in HL-60 cells, phosphodiester ODN were internalized in nonacidic compartments (referred to as “shallow compartments”), whereas phosphorothioate ODN were internalized into acidic compartments. The internalization process of various modified ODN depends on the cell type as well as the nature of the odn (3, 23). The behavior of odn-p-KDEL was thus clearly different from that of ODN carried by glycosylated carriers (neoglycoproteins), which are internalized via membrane lectins and subsequently found in acidic compartments (12, 13, 38).

Laser scanning confocal microscopy analysis was used to study the cellular location of odn, odn-p-KDEA, and odn-p-KDEL by coinubating fluorophore-labeled (*F*-odn or *R*-odn) and oligonucleotides. The nature of the fluorophore tag

did not affect the localization of odn or oligonucleotides. The absence of effect of these tags is in agreement with the data reported by Tonkinson and Stein (23), who showed that the efflux rates of *F*-odn and *R*-odn were identical. To further identify the structures in which odn-p-KDEL was located, we exploited a temperature shift that slows down vesicular transport and results in the compaction of the IC (34, 35). The distinct location of odn and odn-p-KDEL was better demonstrated under these conditions. After a 3-hr chase at 15°, odn-p-KDEL was found close to the nucleus, whereas peptide-free odn were distributed throughout the cytoplasm.

To formally identify the KDEL/ERGIC compartment, we further used immunolabeling with an anti-ERGIC 53 antibody and an anti-KDEL receptor antibody. The odn-p-KDEL and ERGIC-53 were both localized in a perinuclear area, whereas odn-p-KDEA showed no overlap with ERGIC-53. Griffiths *et al.* (16) have shown that the IC is enriched in KDEL proteins recognized by the KDEL receptor. Furthermore, using an anti-KDEL receptor antibody, we demonstrated that although odn-p-KDEL was clearly localized into the compartments labeled by the anti-KDEL receptor antibodies, peptide-free odn and odn-p-KDEA were not localized within the compartments containing KDEL receptors.

Our data suggest that oligonucleotides that end with a KDEL motif can be transported from the cell surface to or close to the ER. Such an internalization pathway is supported by morphological studies showing the presence of the KDEL receptor in TGN (16) and more direct evidence of KDEL receptor-mediated retrograde transport from TGN to ER (39). Miesenböck and Rothman (39) showed that a KDEL-ending peptide containing an *N*-glycosylation site linked through a disulfide bridge to an anti-TGN 38 immunoglobulin was targeted to the TGN because of the anti-TGN (38) antibody. The peptide was released in the TGN from the antibody on reduction of the disulfide bridge and then reached the ER, as demonstrated by a significant acquisition of *N*-linked oligosaccharides for which the transferase is known to be located in the ER.

Our results also indicate that the intracellular fates of odn and odn-p-KDEL are different. The observed rapid efflux of phosphodiester odn is in agreement with the results of other studies (22, 23). In contrast, the KDEL sequence efficiently routes phosphodiester odn from early endosomes to organelles containing the KDEL receptor, the IC, or nearby structures and also slows down the efflux. The efflux of odn-p-KDEA, which is not routed to internal compartments containing the KDEL receptor, is also slowed down. This suggests that the increased efficiency of odn-p-KDEL is in part due to a decrease of their efflux in addition to their localization in a more leaky compartment that is suitable for cytosol delivery.

The compartment from which peptide-free or peptide-linked odn are translocated into the cytosol remains unknown. Despite their identical overall uptake and efflux behaviors, the higher biological activity of odn-p-KDEL compared with that of odn-p-KDEA suggests the crucial role of the KDEL signal sequence in the intracellular trafficking of odn-p-KDEL. It is worth noting that such a retrograde pathway and an increased efficiency were also observed for toxins bearing a KDEL motif compared with the cytotoxicity of the holotoxin and the toxin bearing a KDEA sequence (18). Our data suggest that odn-p-KDEL do not cross a membrane

at the level of early endosomes or along the pathway to lysosomes but rather cross a membrane along the pathway toward the ER, possibly at the level of the IC between the Golgi and the ER, at which it is preferentially retained. Questions concerning the nature of the compartments from where odn-p-KDEL were translocated to the cytosol are being addressed in work in progress.

#### Acknowledgments

We are grateful to Dr. Hans-Peter Hauri (Biozentrum, Basel) and Dr. Bor Luen Tang (National University of Singapore) for their generous gifts of specific antibodies. We thank Dr. Nguyen Thuong for his help in odn synthesis, Dr. Anne-Marie Aubertin (Institut de Virologie, Strasbourg) for her gift of the *pRET-luc* plasmid, Emmanuelle Mothes for synthesis of the peptides, Yves Aubert for preparation of modified odn, and Marie-Thérèse Bousser and Suzanne Nuques for the cell culture. We thank Dr. Patrick Midoux, Dr. Alice Dautry-Varsat, and Dr. Hans Peter Hauri for helpful discussions.

#### References

- Hélène, C., and J. J. Toulmé. Specific regulation of gene expression by antisense, sense and antigen nucleic acids. *Biochim. Biophys. Acta* **1049**: 99–125 (1990).
- Stein, C. A., and Y. C. Cheng. Antisense oligonucleotides as therapeutic agents: is the bullet really magical? *Science (Washington D. C.)* **261**:1004–1012 (1993).
- Stein, C. A., and J. S. Cohen. Oligodeoxynucleotides as inhibitors of gene expression: a review. *Cancer Res.* **48**:2659–2668 (1988).
- Capaccioli, S., G. Di Pasquale, E. Mini, T. Mazzei, and A. Quattrone. Cationic lipids improve antisense oligonucleotide uptake and prevent degradation in cultured cells and in human serum. *Biochem. Biophys. Res. Commun.* **197**:818–825 (1993).
- Kabanov, A. V., S. V. Vinogradov, A. V. Ovcharenko, A. V. Krivonos, N. S. Melik-Nubarov, V. I. Kiselev, and E. S. Severin. A new class of antiviral antisense oligonucleotides combined with a hydrophobic substituent effectively inhibit influenza virus reproduction and synthesis of virus-specific protein in MDCK cells. *FEBS Lett.* **259**:327–330 (1990).
- Lemaitre, M., B. Bayard, and B. Lebleu. Specific antiviral activity of a poly (L-lysine)-conjugated oligodeoxyribonucleotide sequence complementary to vesicular stomatitis virus N protein mRNA initiation site. *Proc. Natl. Acad. Sci. USA* **84**:648–652 (1987).
- Leonetti, J. P., P. Machy, G. Degols, B. Lebleu, and L. Leserman. Antibody-targeted liposomes containing oligodeoxyribonucleotides complementary to viral RNA selectively inhibit viral replication. *Proc. Natl. Acad. Sci. USA* **87**:2448–2451 (1990).
- Wagner, R. W. Gene inhibition using antisense oligodeoxynucleotides. *Nature (Lond.)* **372**:333–335 (1994).
- Zamecnik, P. C., and M. L. Stephenson. Inhibition of Rous sarcoma virus replication and cell transfection by a specific oligodeoxynucleotide. *Proc. Natl. Acad. Sci. USA* **75**:280–284 (1978).
- Goodchild, J., S. Agrawal, M. P. Civeira, P. S. Sarin, D. Sun, and P. C. Zamecnik. Inhibition of HIV replication by antisense oligodeoxynucleotides. *Proc. Natl. Acad. Sci. USA* **85**:5507–5511 (1988).
- Agrawal, S., and J. Y. Tang. Gem-91: an antisense oligonucleotide phosphorothioate as a therapeutic agent for AIDS. *Antisense Res. Dev.* **2**:261–266 (1992).
- Bonfils, E., C. Depierreux, P. Midoux, N. T. Thuong, M. Monsigny, and A. C. Roche. Drug targeting synthesis and endocytosis of oligonucleotide-neoglycoprotein conjugates. *Nucleic Acids Res.* **20**:4621–4629 (1992).
- Sdiqui, N., K. Arar, P. Midoux, R. Mayer, M. Monsigny, and A. C. Roche. Inhibition of human mammary cell line proliferation by membrane lectin-mediated uptake of *ha-ras* antisense oligodeoxynucleotide. *Drug Delivery* **2**:63–72 (1995).
- Munro, S., and H. R. B. Pelham. A C-terminal signal prevents secretion of luminal ER proteins. *Cell* **48**:899–907 (1987).
- Tang, B. L., S. H. Wong, X. L. Qi, S. H. Low, and W. Hong. Molecular cloning, characterization, subcellular localization and dynamics of p23, the mammalian KDEL receptor. *J. Cell Biol.* **120**:325–328 (1993).
- Griffiths, G., M. Ericsson, J. Krijnse-Locker, T. Nilsson, B. Goud, H. D. Söling, B. L. Tang, S. H. Wong, and W. Hong. Localization of the Lys, Asp, Glu, Leu tetrapeptide receptor to the Golgi complex and the intermediate compartment in mammalian cells. *J. Cell Biol.* **127**:1557–1574 (1994).



17. Seetharam, S., V. K. Chaudhary, D. FitzGerald, and I. Pastan. Increased cytotoxic activity of *Pseudomonas* exotoxin and two chimeric toxins ending in KDEL. *J. Biol. Chem.* **266**:17376–17381 (1991).
18. Wales, R., L. M. Roberts, and J. M. Lord. Addition of an endoplasmic reticulum retrieval sequence to ricin A chain significantly increases its cytotoxicity to mammalian cells. *J. Biol. Chem.* **268**:23986–23990 (1993).
19. Sandvig, K., O. Garred, K. Prydz, J. V. Kozlov, S. H. Hansen, and B. van Deurs. Retrograde transport of endocytosed Shiga toxin to the endoplasmic reticulum. *Nature (Lond.)* **358**:510–512 (1992).
20. Pastan, I., V. Chaudhary, and D. J. Fitzgerald. Recombinant toxins as novel therapeutic agents. *Annu. Rev. Biochem.* **61**:331–354 (1992).
21. Simpson, J. C., C. Dascher, L. M. Roberts, J. M. Lord, and W. E. Balch. Ricin cytotoxicity is sensitive to recycling between the endoplasmic reticulum and the Golgi complex. *J. Biol. Chem.* **270**:20078–20083 (1995).
22. Marti, G., W. Egan, P. Noguchi, G. Zon, M. Matsukura, and S. Broder. Oligodeoxyribonucleotide phosphorothioate fluxes and localization in hematopoietic cells. *Antisense Res. Dev.* **2**:27–39 (1992).
23. Tonkinson, J. L., and C. A. Stein. Patterns of intracellular compartmentalization, trafficking and acidification of 5'-fluorescein labeled phosphodiester and phosphorothioate oligodeoxynucleotides in HL60 cells. *Nucleic Acids Res.* **22**:4268–4275 (1994).
24. Arar, K., A. M. Aubertin, A. C. Roche, M. Monsigny, and R. Mayer. Synthesis and antiviral activity of peptide-oligonucleotide conjugates prepared by using N<sub>α</sub>-bromoacetyl peptides. *Bioconjugate Chem.* **6**:573–577 (1995).
25. Sorger, P. K., and H. R. B. Pelham. The glucose regulated protein grp94 is related to heat shock protein hsp 90. *J. Mol. Biol.* **194**:341–344 (1987).
26. Midoux, P., C. Mendès, A. Legrand, J. Raimond, R. Mayer, M. Monsigny, and A. C. Roche. Specific gene transfer mediated by lactosylated poly-L-lysine in hepatoma cells. *Nucleic Acids Res.* **21**:871–878 (1993).
27. De Wet, J. R., K. V. Wood, M. De Luca, D. R. Helinski, and S. Subramani. Firefly luciferase gene: structure and expression in mammalian cells. *Mol. Cell. Biol.* **7**:725–737 (1987).
28. Stein, C. A., J. L. Tonkinson, L. M. Zhang, L. Yakubov, J. Gervasoni, R. Taub, and S. A. Rotenberg. Dynamics of the internalization of phosphodiester oligodeoxynucleotides in HL60 cells. *Biochemistry* **32**:4855–4861 (1993).
29. Midoux, P., A. C. Roche, and M. Monsigny. Quantitation of the binding, uptake and degradation of fluoresceinylated neoglycoprotein by flow cytometry. *Cytometry* **8**:327–334 (1987).
30. Monsigny, M., A. C. Roche, and P. Midoux. Uptake of neoglycoproteins via membrane lectin(s) of L1210 cells evidenced by quantitative flow cytometry and drug targeting. *Biol. Cell* **51**:187–196 (1984).
31. Lowry, O. H., N. J. Roseburg, A. L. Farr, and R. J. Randall. Protein measurement with the folin phenol reagent. *J. Biol. Chem.* **193**:265–275 (1951).
32. Johnson, G. D., R. S. Davidson, K. C. McNamee, G. Russell, D. Goodwin, and E. J. Holborow. Fading of immunofluorescence during microscopy: a study of the phenomenon and its remedy. *J. Immunol. Methods* **55**:231–242 (1982).
33. Banerjee, R., K. Sperber, T. Pizzella, and L. Mayer. Inhibition of HIV-1 productive infection in hepatoblastoma HepG2 cells by recombinant tumor necrosis factor  $\alpha$ . *AIDS* **6**:1127–1131 (1992).
34. Kuismäen, E., and J. Sarraste. Low temperature induced transport block as tool to manipulate membrane traffic. *Methods Cell. Biol.* **32**:257–274 (1989).
35. Schweizer, A., J. A. Fransen, K. Matter, T. E. Kreis, L. Ginsel, and H. P. Hauri. Identification of an intermediate compartment involved in protein transport from endoplasmic reticulum to Golgi apparatus. *Eur. J. Cell Biol.* **53**:185–196 (1990).
36. Akhtar, S., and R. L. Juliano. Cellular uptake and intracellular fate of antisense oligonucleotides. *Trends Cell Biol.* **2**:139–158 (1992).
37. Vlassov, V. V., L. A. Balakireva, and L. A. Yakubov. Transport of oligonucleotides across natural and model membranes. *Biochim. Biophys. Acta* **1197**:95–108 (1994).
38. Monsigny, M., A. C. Roche, P. Midoux, and R. Mayer. Glycoconjugates as carriers for specific delivery of therapeutic drugs and genes. *Adv. Drug. Delivery Rev.* **14**:1–24 (1994).
39. Miesenböck, G., and J. E. Rothman. The capacity to retrieve escaped ER proteins extends to the trans-most cisterna of the Golgi stack. *J. Cell Biol.* **129**:309–319 (1995).

---

**Send reprint requests to:** Annie-Claude Roche or Chantal Pichon, Glycobiologie CBM-CNRS, rue Charles Sadron, F-45071 Orléans Cedex 02, France.  
E-mail: roche@cnrs-orleans.fr

---